Polymer-Stabilized Reflective Cholesteric Displays: Effects of Chiral Polymer Networks on Reflectance Properties

Daniel J. Dyer,*,† U. Paul Schröder,*,‡ K.-Pong Chan, and Robert J. Twieg

NSF Center on Polymer Interfaces and Macromolecular Assemblies, IBM Almaden Research Center, 650 Harry Road, San Jose, California 95120

Received February 4, 1997[⊗]

A white reflecting polymer-stabilized cholesteric textured liquid-crystal cell was created by incorporation of chiral methacrylate polymer networks. The position and stereochemical configuration of the chiral centers plays an integral role in the observed reflection spectra. Chiral polymer networks with chiral centers separated from the polymer backbone and that unwind the cholesteric helix pitch produce the broadest reflection band in these LC mixtures.

Introduction

Recently, polymer stabilized cholesteric liquid crystal (PSCT) devices which incorporate mesogenic polymer networks have been described.[1] Reflective liquid-crystal (LC) displays are of particular interest because they do not require polarizers or back-lighting; thus, power consumption is dramatically reduced. For PSCT displays the polymer network serves three functions: First, it stabilizes the scattering focal-conic state. Second, the polymer disperses the Bragg-reflecting planar texture into multidomains with misaligned helix axes. Therefore, the Bragg condition is valid over broader viewing angles. Finally, the polymer network exhibits a "memory" effect which enables faster switching. In particular, we are interested in black-and-white reflective "paperlike" displays which maintain high contrast over a wide range of viewing angles.[2] Two approaches have been used in the past in order to produce a white reflecting color. The scattering mode utilizes backscattering in the focal-conic texture, and the Bragg reflecting mode takes advantage of a reflection peak in the planar texture of the cholesteric liquid crystal. In this paper we will focus on Bragg reflecting systems. The black color is achieved by placing a black absorbing layer behind the cell. By switching the cell to a weakly scattering focal-conic texture or to the transparent homeotropic texture, the background becomes visible and the cell appears black.

It is useful to understand the origin of the Bragg-reflected light in order to design improved systems. For a planar aligned cholesteric LC cell the helix pitch is oriented normal to the surface. Incident light is split into two circular components, one of which will be reflected and the other transmitted. The wavelength of Bragg reflected light (λ) is equal to the product of the average refractive index (n) and the helix pitch (p), (i.e., $\lambda = np$). The bandwidth of this reflected light ($\Delta\lambda$) is given by $\Delta\lambda = \Delta n\lambda/n$, where Δn is the birefringence of the liquid crystal. Generally, the reflection peak is very sharp and gives rise to brilliant colors. However, to produce a bright "white" color, the bandwidth of the reflection must be significantly increased over the entire visible range. Since the bandwidth is proportional to the birefringence of the liquid crystal, it may be useful to incorporate highly birefringent materials. But large Δn LCs will also increase light scattering at domain boundaries and may lead to a lighter shade of black in the focal-conic texture due to excess backcattered light, thus decreasing the contrast of the device.

Increasing liquid-crystal birefringence is not the only way to broaden the reflection band. For instance, the polymer network could be used to increase $\Delta\lambda$ by affecting the helix pitch locally. As a result, the bandwidth of the reflected light will be a function of the distribution of helix pitch lengths in the cell. It is known that the incorporation of chiral centers in the polymer network can broaden the reflection bandwidth.[3] However, until now the influence of chiral networks on the bulk cholesteric LC, and the observed reflection band has not been systematically explored. From the results of previous investigations it can be assumed that the polymer network and the LC undergo phase separation during polymerization. At least a large fraction of the polymer resides in phase-separated structures of fractal morphology.[4] Consequently, only the polymer

† Current address: The Beckman Institute, California Institute of Technology, Pasadena, CA 91125.

‡ Current address: Universität Stuttgart, Institut für Textil-und Faserchemie, Pfaffenwaldring 55, 70550 Stuttgart, Germany.

⊗ Abstract published in *Advance ACS Abstracts,* June 15, 1997.

(1) (a) Doane, J. W.; Yang, D.-K.; Pfeiffer, M. *Macromol. Symp.* **1995**, *96*, 51−60. (b) Doane, J. W.; Yang, D.-K.; Chien, L.-C. *Liquid Crystalline Light Modulating Device and Material*; Kent State University: Kent, OH, 1995; US Patent 5437811. For reviews on polymer dispersed liquid crystals see: (c) Bouteiller, L.; Le Barney, P. *Liq. Cryst.* **1996**, *21*, 157−174. (d) Drzaic, P. S. *Liquid Crystal Dispersions*; World Scientific Publishing Co. Pte. Ltd.: Singapore, 1995; Vol. 1.

(2) (a) Held, G. A.; Kosbar, L. L.; Lowe, A. C.; Afzali-Ardakani, A.; Schröder, U. P.; Chan, K.-P.; Russell, T.; Twieg, R. J.; Miller, R. D. *Relationship Between Network Structure and the Electrooptical Properties of Polymer Stabilized Cholesteric Textures*, SID Euro 96; Conference in Birmingham England; pp 573−576, 1996. (b) Yang, D.-K.; West, J. L.; Chien, L.-C.; Doane, J. W. *J. Appl. Phys.* **1994**, *76*, 1331−1333. (c) Yang, D.-K.; Doane, J. W. *SID 92 Digest* **1992**, 759−761. (d) Leroux, N.; Chien, L.-C. *White Reflective Polymer Stabilized Cholesteric Displays*; Proceedings of American Chemical Society Spring Meeting; Division of Polym. Mater. Sci. Eng.; Anaheim, CA USA, 1995; Vol. 72, pp 285−286.

(3) Chien, L.-C.; Nabor, M.-F.; Müller, U.; Leroux, N.; Yang, D.-K.; Doane, J. W.; Boyden, M. N.; Walz, A. J.; Citano, C. M. *Recent Advances in Materials for Polymer Stabilized Liquid Crystals*; National Meeting of the American Chemical Society, Anaheim, CA; American Chemical Society: Washington DC, 1995; Division of Polym. Mater. Sci. Eng., Vol. 72, pp 492−493.

S0897-4756(97)00070-7 CCC: $14.00

Table 1. Structures of Monomers and Liquid-Crystalline Materials

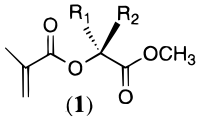

(**1**)

1	R_1	R_2	Stereocenter
a	CH_3	H	R
b	H	CH_3	S
c	H,CH_3	H,CH_3	Racemic
d	H	H	Achiral

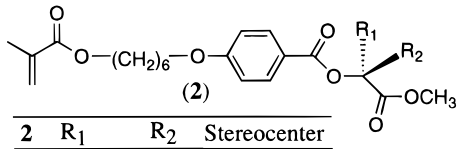

(**2**)

2	R_1	R_2	Stereocenter
a	CH_3	H	R
b	H	CH_3	S
c	H,CH_3	H,CH_3	Racemic
d	H	H	Achiral

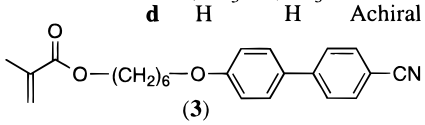

(**3**)

ZLI-4572 = Chiral LC from E. Merck (Hawthorne NY, USA), also known as (R1011)
CB15 = Chiral Cyanobiphenyl LC from BDH LTD (Poole, England)
RM206 (Reactive Mesogen 206) = Diacrylate Phenylbenzoate LC from BDH LTD (Poole,England)
E48 = Nematic LC mixture composed of cyanobiphenyls from BDH LTD (Poole, England)
BME (Benzoin methyl ether) = photointiator usually added as a 10% solution in toluene

that resides at the interface of such a structure can interact with the liquid crystal. This implies that the distance of the chiral center from the polymer backbone could play an important role in influencing the bulk LC and the reflection band.

We have investigated the influence of the position of the chiral centers in the side group of functionalized polymers with respect to the polymer backbone on the reflection properties of polymer stabilized cholesteric liquid crystals. In addition, we have examined the influence of the handedness of the chiral centers on the bulk cholesteric helix pitch which is locally unwound or compressed depending on the particular enantiomer. It is unclear whether the positioning of the chiral center or the handedness is more effective at broadening the reflection bandwidth. Herein we present results on experiments with polymer networks prepared from monomers with different nonchiral, racemic, and enantiomeric functional groups.

Experimental Section

The materials used in the LC−monomer mixtures are described in Table 1. A green reflecting cholesteric stock solution ($\lambda_{max} \sim 525$ nm) was composed of 3.6% ZLI-4572, 24.8% CB15, and 71.6% E48. The yellow reflecting cholesteric stock solution ($\lambda_{max} \sim 575$ nm) was composed of 4% ZLI-4572, 18.5% CB15, and 77.5% E48. Individual reactive LC mixtures and cells were made as follows: First, into a small vial were placed chiral monomer **1a** (7.350 mg), methacrylate **3** (3.675 mg),[5] diacrylate **RM206** (3.675 mg), stock green cholesteric mixture (285.0 mg), and approximately 15 mg of a 10 wt % solution of BME in toluene. The contents were briefly heated above the isotropic point and then dried overnight at room temperature under vacuum to yield a mixture that was 5% reactive monomer and 95% cholesteric LC. The contents were then heated once again to the isotropic point and mixed thoroughly. The LC mixture was cooled to room temperature and then commercially available 25 μm ITO cells[6] coated with a rubbed planar polyimide alignment layer were filled under vacuum. The filled cell was pressed slightly to expel excess fluid and then sealed with epoxy. The cell was then annealed by briefly heating to the isotropic state (~70 °C) and then allowing the cell to cool before the reflectance spectrum was taken prior to polymerization.

During irradiation the liquid-crystal cell was placed 15 cm from the lamp and covered with a 0.5 mm gelatin neutral density filter. The cell was irradiated at 365 nm for 5.5 h with an intensity of 1.72 mW/cm^2. The intensity was controlled with a Model 770 intensity controller from Optical Associates, Inc. (OAI), Santa Clara, CA. Reflectance measurements were performed on a Minolta spectrophotometer (Model CM-100), equipped with a silicon photodiode array detector and spectral filter array. The reflection mode was calibrated to a white background using a Minolta CM-A11 calibration plate. All measurements were taken at 0° viewing angle (i.e., normal to the surface).

All starting materials were purchased from Aldrich Chemicals and used without purification. The NMR spectra was taken on a Bruker AM-250 spectrometer. Representative syntheses and spectra of new compounds are listed below.

(*R*)-Methyl-2-[(2-methyl-1-oxo-2-propenyl)oxy]propanoic Acid (1a). Diethylazodicarboxylate (5.01 g, 28.8 mmol) was added to a stirred solution of (*S*)-methyl lactate (2.0 g, 19.2 mmol), methacrylic acid (1.65 g, 19.2 mmol), and triphenylphosphine (7.55 g, 28.8 mmol) in 200 mL of anhydrous THF. The reaction mixture was stirred overnight and was then concentrated and filtered. The filtrate was purified via flash chromatography over silica gel by eluting with a 90/10 solution of hexanes/ethyl acetate. Evaporation of solvent yielded 1.825 g (55%) of a colorless oil: R_f 0.37 (90/10 hexanes/ethyl acetate); ^{1}H NMR (250 MHz, $CDCl_3$) δ 1.51 (d, $J = 7.04$, 3H), 1.94 (s, 3H), 3.73 (s, 3H), 5.12 (q, $J = 7.08$, 1H), 5.61 (m, 1H), 6.18 (m, 1H).

Methyl-2-[(2-methyl-1-oxo-2-propenyl)oxy]ethanoic acid (1d). Diethylazodicarboxylate (4.833 g, 27.75 mmol) was added to a stirred solution of methyl glycolate (2.0 g, 22.2 mmol), methacrylic acid (1.911 g, 22.2 mmol), and triphenylphosphine (7.279 g, 27.75 mmol) in 150 mL of anhydrous THF. The reaction mixture was stirred overnight and was then adsorbed onto silica gel and purified via flash chromatography over silica gel with gradual elutions from 95/5 to 80/20 (hexanes/ethyl acetate). Evaporation of solvent yielded 2.98 g (85%) of a colorless oil: ^{1}H NMR (250 MHz, $CDCl_3$) δ 1.96 (s, 3H), 3.74 (s, 3H), 4.66 (s, 2H), 5.63 (m, 1H), 6.20 (m, 1H).

4-[[6-[(2-methyl-1-oxo-2-propenyl)oxy]hexyl]oxy]benzoic acid [(*R*)-Methyl (2-propanoic acid)] Ester (2a). Diethylazodicarboxylate (310 mg, 1.78 mmol) was added to a stirred solution of (*S*)-methyl lactate (163 mg, 1.57 mmol), benzoic acid derivative **4**[7] (437 mg, 1.43 mmol), and triphenylphosphine (467 mg, 1.78 mmol) in 14 mL of anhydrous THF. The reaction mixture was stirred overnight and was then

(4) Fung, Y. K.; Yang, D.-K.; Ying, S.; Chien, L.-C.; Zumer, S.; Doane, J. W. *Liq. Cryst.* **1995**, *19*, 797−801, and ref 2a.
(5) The synthesis of this monomer will be described elsewhere.
(6) The 25 μm thick (3 cm × 3 cm) cells were purchased from Crystaloid, 5282 Hudson Drive, Hudson, OH 44236.
(7) Sastri, S. B.; Stupp, S. I. *Macromolecules* **1993**, *26*, 5657−5663.

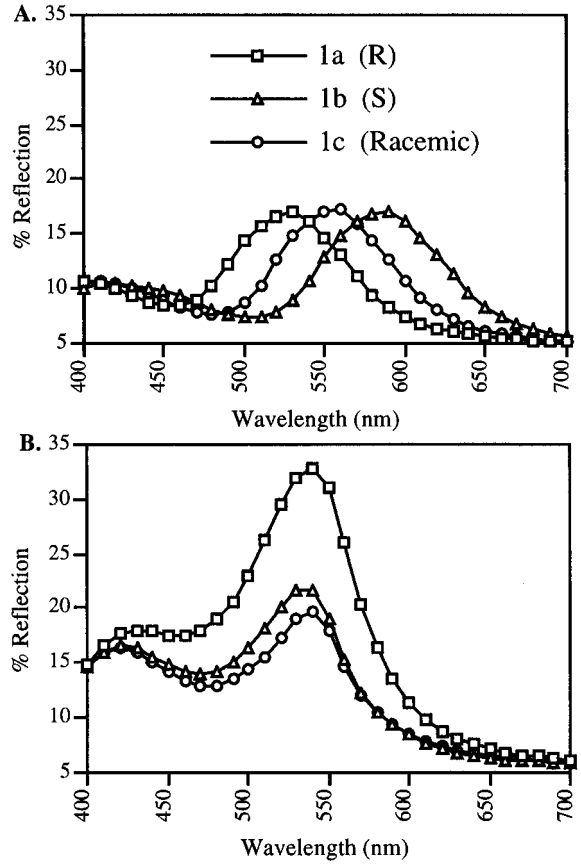

Figure 1. (A) Reflectance spectra *before* polymerization with monomers **1a**−**c**. (B) Reflectance spectra *after* polymerization and annealing with monomers **1a**−**c**.

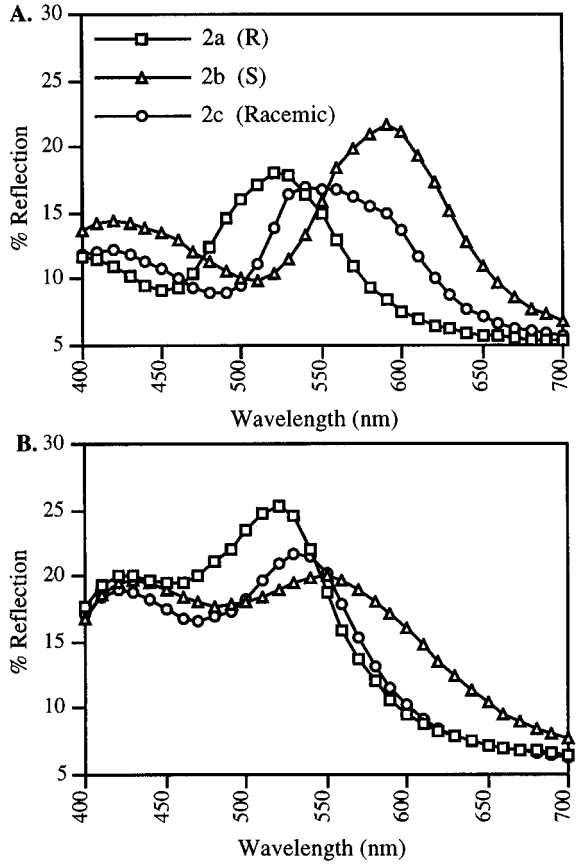

Figure 2. (A) Reflectance spectra *before* polymerization with monomers **2a**−**c**. (B) Reflectance spectra *after* polymerization and annealing with monomers **2a**−**c**.

adsorbed onto silica gel and purified via flash chromatography over silica gel with gradual elutions from 80/20 to 65/35 (hexanes/ethyl acetate). Evaporation of solvent yielded 90 mg (16%) of a colorless oil. An additional 250 mg of slightly impure product was also recovered: ^{1}H NMR (250 MHz, $CDCl_3$) δ 1.35 (m, 4H), 1.59 (d, J = 7.06, 3H), 1.65−1.83 (m, 4H), 1.92 (m, 3H), 3.74 (s, 3H), 4.00 (t, J = 6.41, 2H), 4.14 (t, J = 6.58, 2H), 5.28 (q, J = 7.06, 1H), 5.52 (m, 1H), 6.07 (m, 1H), 6.89 (d, 2H), 8.00 (d, 2H).

4-[[6-[(2-Methyl-1-oxo-2-propenyl)oxy]hexyl]oxy]benzoic Acid [Methyl-(2-ethanoic acid)] Ester (2d). Diethylazodicarboxylate (710 mg, 4.08 mmol) was added to a stirred solution of methyl glycolate (323 mg, 3.59 mmol), benzoic acid derivative **4**[7] (1.0 g, 3.26 mmol), and triphenylphosphine (1.07 g, 4.08 mmol) in 33 mL of anhydrous THF. The reaction mixture was stirred overnight and was then adsorbed onto silica gel and purified via flash chromatography over silica gel with gradual elutions from 80/20 to 65/35 (hexanes/ethyl acetate). Evaporation of solvent yielded 1.13 g (92%) of a colorless oil: ^{1}H NMR (250 MHz, $CDCl_3$) δ 1.35−1.55 (m, 4H), 1.60−1.86 (m, 4H), 1.92 (m, 3H), 3.76 (s, 3H), 4.00 (t, J = 6.40, 2H), 4.14 (t, J = 6.50, 2H), 4.81 (s, 2H), 5.52 (m, 1H), 6.07 (m, 1H), 6.89 (d, 2H), 8.00 (d, 2H).

Results and Discussion

Two series of chiral monomers (**1a**−**c** and **2a**−**c**) were synthesized in order to determine the effects of enantiomers and racemates on reflection characteristics relative to achiral monomers (**1d** and **2d**). Figure 1a shows that before polymerization the monomers mix well with the LC host, exhibiting a smooth transition in λ_{max} from the *R* to *S* compounds. Furthermore, the peak widths and intensities are nearly identical before polymerization when the monomers are randomly dispersed throughout the cell. Figure 1b after polymerization illustrates two important concepts: first, the reflection intensities generally increase after polymerization and in the case of the *R* enantiomer exhibits a larger change relative to the other two. Previous results show that the reflected intensity increases with polymer concentration to an optimum and then falls at higher polymer concentrations.[8] The increase in reflected intensity is believed to result from increasing the number of domains with misaligned helixes. However, large polymer concentrations decrease the intensity because the volume density at the Bragg angle decreases.[8] Clearly the *R* enantiomer (**1a**) creates more reflective domains than the racemate or *S* enantiomer. This effect cannot be attributed to polymer concentration because that was identical for each cell (~5%); however, the number and size of the domains may be different, but this was not examined here. Second, the λ_{max} of all three cells is nearly identical after polymerization. This is indicative of a nearly 100% phase separation of the polymer network from the bulk LC because the enantiomers exhibit different λ_{max} before polymerization but not after. It has always been assumed that the polymer network was completely phase separated; however, these results are the first noninvasive confirmation of phase separation. Previous studies that examined the miscibility of polymer networks in LCs relied on invasive techniques to extract the LC from the polymer network, which may influence the network structure.[9]

(8) Fritz, W. J.; St. John, W.; Yang, D.-K.; Doane, J. W. *SID Digest 94* **1994**, 841−844.

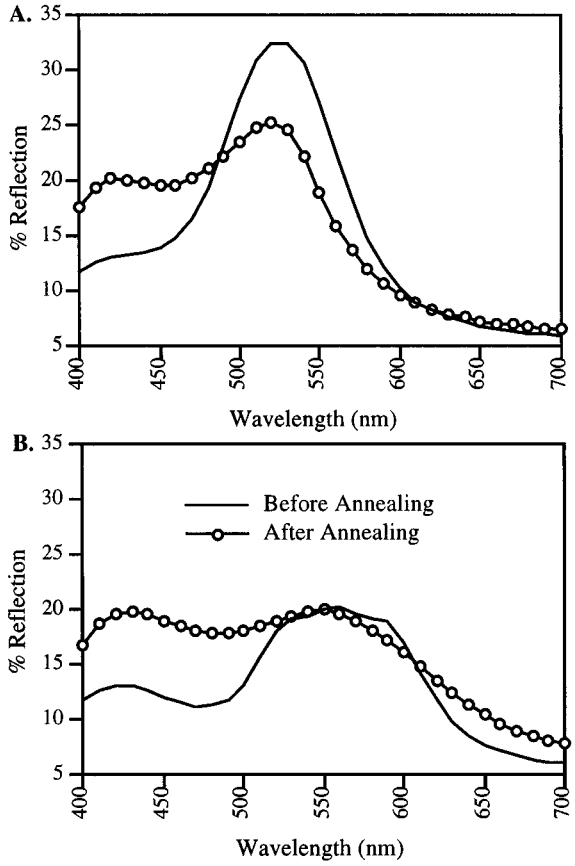

Figure 3. Effect of annealing after polymerization on reflectance spectra. (A) Reflectance spectra before and after annealing of *R* enantiomer **2a**. (B) Reflectance spectra before and after annealing of *S* enantiomer **2b**.

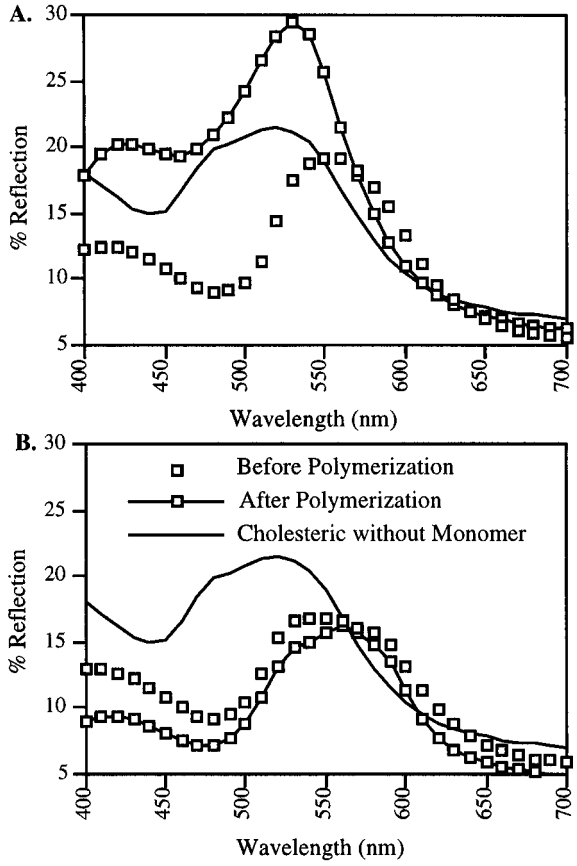

Figure 4. (A) Reflectance spectra before and after polymerization and annealing with achiral monomer **1d**. (B) Reflectance spectra before and after polymerization and annealing with achiral monomer **2d**. The reflectance spectra of the green cholesteric stock solution is added for reference.

For monomers (**1a**−**c**) the chiral methyl lactate moiety is located close to the polymer backbone. Therefore, the *phase-separated* chiral centers in the polymer are anticipated to have little influence on the reflectance bandwidth and the bulk cholesteric helix pitch. We felt that by placing the methyl lactate moiety further from the polymer backbone, we would affect a greater change in the bulk helix pitch and bandwidth because the stereocenters should mix better with the bulk LC. Figure 2 supports this hypothesis, indicated by the different λ_{max} for the three monomers *after* polymerization. In addition, the reflection intensity for the *S* enantiomer (**2b**) is nearly constant from 400 to 600 nm (Figure 2b). The binodal spectra may be the result of Bragg reflection from both polymer-rich and polymer-deficient domains that possess different helix pitches. Interestingly, the spectra intensities before polymerization are not as uniform as in Figure 1a; however, the λ_{max} for monomers **1a**−**c** and **2a**−**c** are nearly identical for respective stereocenters before polymerization. As illustrated in Figure 2b, the *R* enantiomer (**2a**) exhibits a larger reflectance intensity at λ_{max} than **2b** or **2c** after polymerization. This is similar to previous results with compound **1a** described in Figure 1b. Furthermore, the color of the cell containing **2b** appears whiter than the other cells, which exhibit a light green color. Finally, the cells illustrated in Figure 2b appear to be more homogeneous under polarized optical microscopy than the cells from Figure 1b, which exhibit thin polymer fibers throughout the cell. However, the texture of all cells is similar when viewed with the naked eye.

In general, annealing of the LC cells after polymerization yields smoother reflection curves when compared to nonannealed cells. This may result from the healing of defects between liquid-crystalline domains that were present before annealing. However, heating to the isotropic point may also affect polymer−LC domain boundaries. Although we did not determine the glass transition temperature (T_g) for the polymer networks, it is reasonable to assume that at the annealing temperature (~70 °C) the structure of the polymer network may be altered. The annealing process leads to broader reflection bandwidths as described in Figure 3. In particular, the peak near 420 nm becomes more intense after annealing for nearly all examples cited in this paper, as illustrated in Figure 3 for enantiomers **2a** and **2b**. Annealing likely heals defects between individual domains and may also increase the Bragg reflection of domains with high polymer concentration leading to the observed growth near 420 nm. In addition, the annealing process may yield a more isotropic polymer network which increases the number of domain boundaries, thereby increasing the scattering at lower wavelengths. Alternatively the chiral polymer network may possess a helical structure which selectively reflects light at lower wavelengths. Upon heating to the clearing point,

(9) (a) Fung, Y. K.; Yang, D.-K.; Ying, S.; Chien, L.-C.; Zumer, S.; Doane, J. W. *Liq. Cryst.* **1995**, *19*, 797−801. (b) Heynderickx, I.; Broer, D. J.; Tervoort-Engelen, Y. *J. Mater. Sci.* **1992**, *27*, 4107−4114. (c) Hikmet, R. A. M.; Zwerver, B. H. *Liq. Cryst.* **1992**, *Vol. 12*, 319−336. (d) Smith, G. W. *Phys. Rev. Lett.* **1993**, *70*, 198−201. (e) Shimada, E.; Uchida, T. *Jpn. J. Appl. Phys.* **1992**, *31*, L352-L354. (f) Hikmet, R. A. M. *J. Appl. Phys.* **1990**, *68*, 4406−4412.

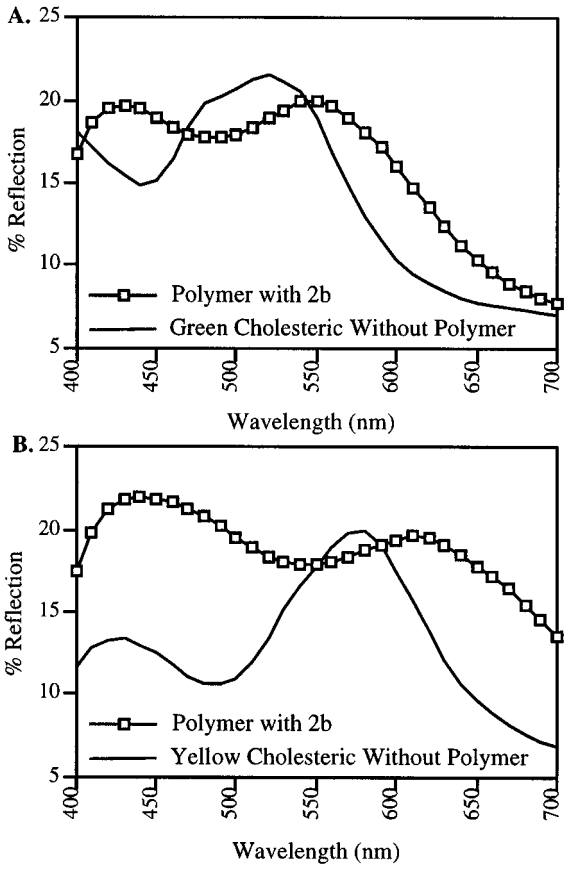

Figure 5. Effect of cholesteric helix pitch on reflectance. (A) Reflectance spectra of polymer network containing **2b** and green cholesteric LC. (B) Reflectance spectra of polymer network containing **2b** and yellow cholesteric LC.

all peaks disappear and the reflection intensity approaches zero, which suggests that the observed growth near 420 nm is not solely due to the polymer network, nor is it due to reflection from the ITO−LC interface.

Achiral monomers **1d** and **2d** were synthesized in order to examine the difference between chiral and achiral polymer networks with similar steric properties. In **1d** and **2d** the achiral methyl glycolate moiety was incorporated into the monomer which is similar sterically to the chiral methyl lactate moiety used previously. Figure 4 illustrates that both achiral polymer networks exhibit a substantial influence on the reflectance spectra when compared to the cholesteric green LC mixture without any monomer. In addition, neither **1d** nor **2d** effect a significant change in the spectra after polymerization. Furthermore, the reflectance spectra of the nonchiral polymer networks are quite similar to their respective racemic networks **1c** and **2c** as described in Figures 1 and 2, respectively. This confirms that the chirality of the polymer networks plays an integral role in the overall reflectance characteristics.

The ultimate goal of our work is to create a white reflective cholesteric LC cell. The results described in Figure 5a show a cell with a broad reflection bandwidth. However, the reflectance tails off sharply at ~575 nm. This leads to a very light green tint to the cell when viewed under ambient light. We felt that by changing the pitch of the cholesteric LC from a green to a yellow reflecting mixture, we might be able to stretch the large reflection band beyond 650 nm. Figure 5b shows that this strategy was quite successful. The *S* enantiomer **2b** is very effective at increasing the reflection bandwidth regardless of the helix pitch of the cholesteric LC mixture. Indeed, this cell appears very white under normal lighting conditions. However, the reflectance intensity must be improved further in order to obtain satisfactory contrast for a practical commercial display.

Conclusions

Locally induced changes of the helix pitch of cholesteric liquid crystals can be affected by chiral polymer networks. Since the polymer forms a structure which is phase-separated from the bulk LC, the control of properties at the polymer−LC interface are important. As a consequence, it appears that the chiral centers of the polymer must be well separated from the polymer backbone in order to maintain the influence of the chiral centers on the liquid crystal after polymerization. It has been shown that there is a clear distinction between different enantiomers of the polymer network on the reflection properties. The enantiomer which decreases the pitch of the cholesteric helix locally leads to improved reflection properties compared to the other enantiomer or racemate. The origin of the second reflection peak at 420 nm during polymerization and annealing is unclear but may play an important role in the design of white reflective cholesteric LC displays. Finally, a significant broadening of the reflection band was observed, producing a white reflecting LC cell.

Acknowledgment. The authors wish to thank A. C. Lowe and J. Gordon of IBM for an insightful discussion of the results. This work was supported by the National Science Foundation Materials Research Science and Engineering Center on Polymer Interfaces and Macromolecular Assemblies under the cooperative agreement No. NSF-DMR 9400354.

CM970070D